Arch. Metall. Mater. **68** (2023), 4, 1319-1326

DOI: https://doi.org/10.24425/amm.2023.146197

YU-LAI SONG[1,2], ZHI-HE DOU[2*], TING-AN ZHANG[2], CHU CHENG[3], HUI FANG[4], CHAO-LEI BAN[1]

THERMODYNAMIC INSIGHT INTO THE EQUILIBRIUM COMPONENT PREDICTION IN THE Al-Ti-Ca-OXIDE SYSTEM

The prediction of equilibrium components for chemical reactions is a considerable section in the metallurgical industry. According to the ion and molecule coexistence theory (IMCT), a modified mass action concentration model based on a thermodynamic database is proposed in this paper, which complys with the law of mass conservation and can be applied in the batching process for Al-Ti-Ca-oxide system that originates from SHS (Self-propagating High-temperature Synthesis) metallurgy. The trend for slag and alloy component under different batching conditions are in good agreement with experiment, while the difference between the theoretical calculation and experiment can be attributed to the deviation from the thermodynamic equilibrium. The modified mass action concentration model with melts and slag can be used to predict the composition and content of the system when equilibrium is achieved at a certain temperature under a specific material ratio, which is conducive to reducing the cost of the experiment and predicting the operability of the actual process. Moreover, it is believed that this thermodynamic insight may has certain application prospects in these metallurgical procedure based on the equilibrium process.

Keywords: metallurgy; ion and molecule coexistence theory; thermodynamics; equilibrium; slag

1. Introduction

The prediction of the equilibrium component of a collection of chemical reactions is such momentous that it can reduce the capitalized cost investment and can also be utilized to explore the critical information required for practical application [1-3]. Usually, to obtain the optimal raw material ratio of a certain reaction process, a large number of experiments across different raw material ratio ranges are processed to obtain the influence of some elements affecting the reaction process. However, this general route for searching for the optimal conditions displays defective characteristics, and a suitable prognosis seems to be a better choice in the process of metallurgy, material and chemical synthesis.

For the metallurgical process of extracting valuable components from minerals, effective separation from byproducts is usually accompanied. To date, many measures have been taken to study the potential mechanism underlying the reaction process, including experimental characterization, theoretical speculation and computational simulation [4-7]. Currently, model prediction is a prevailing route because it is characterized by fleetness, time-savings and efficiency. In recent years, the mass action concentration model based on the ion and molecular coexistence theory has been widely used in the calculation of the structure and activity of multicomponent slag in metallurgical systems, as well as the influence of a single factor on the process. Zuo et al. [8] studied the effects of CaO on the reduction of copper slag by biomass based on ion and molecule coexistence theory and thermogravimetric experiments. Tang et al. [9] established the mass action concentration model of CaO-MgO-FeO-Al_2O_3-SiO_2 slag systems and discussed the effect of slag basicity, aluminum content in molten steel, degree of vacuum and furnace lining on the magnesium content in molten steel and eventually acquired the formation mechanism of $MgO \cdot Al_2O_3$ spinel-type inclusions in casting steel. Wang et al. [10] created the quaternary slag system CaO-SiO_2-Al_2O_3-MgO calculation model to analyze the deoxidation and desuphurization ability for refining bearing steel, the effect on the morphology of inclusions and a comparison with experiments. Moreover, the mass action concentration theory can also be used to study the thermodynamic properties of melts, solid solutions and aqueous solutions [11-17]. According to the phase

[1] LIAOCHENG UNIVERSITY, SCHOOL OF MATERIALS SCIENCE AND ENGINEERING, LIAOCHENG, SHANDONG, 252059 P.R. CHINA
[2] NORTHEASTERN UNIVERSITY, MINISTRY OF EDUCATION, KEY LABORATORY OF ECOLOGICAL METALLURGY OF MULTI-METAL INTERGROWN ORES, SHENYANG, LIAONING, 110819 P.R. CHINA
[3] HENAN UNIVERSITY OF SCIENCE AND TECHNOLOGY, SCHOOL OF MATERIALS SCIENCE AND ENGINEERING, LUOYANG, HENAN, 471003, P.R. CHINA
[4] LONGKOU DONGHAI ALUMINA CO., LTD. NANSHAN GROUP, YANTAI, SHANDONG, 265071, P.R. CHINA

* Corresponding author: douzh@smm.neu.edu.cn

diagrams, measured activities and the coexistence theory, as well as the appearance of mixing free energy and maxima of excess free energy, Zhang [11-15] calculated the structural units and action concentrations of various binary and ternary metallic melts and solutions, and the results show excellent agreement with the measured values. Meanwhile, the thermodynamic parameters can reflect the intrinsic structural characteristics of relevant melts. Moreover, based on the ion and molecule coexistence theory (IMCT), a thermodynamic model of calculating mass action concentrations for structural units or ion couples in $NaClO_4$-H_2O and NaF-H_2O binary solutions and $NaClO_4$-NaF-H_2O ternary strong electrolyte aqueous solutions was developed by Yang et al. [16]. The calculated results revealed that the mass action concentrations of structural units or ion couples strictly follow the mass action law. From the standpoints mentioned above, the mass action and concentration law can also be used to predict the chemical equilibrium at a certain temperature, including the possible structural units and their relevant contents. As many industrial processes are always accompanied by the oxidation-reduction and separation of substances, the prediction of the equilibrium process and trend can effectively assess the relationship between the initial and final states, especially for metallurgical, chemical and biosynthetic processes, which usually require considerable time and investment costs. Therefore, it is necessary to establish a mass action equilibrium concentration model to predict the relationship between the proportion of ingredients and the composition of products. Suitable preconditions can be quickly obtained and the experimental investment can be saved through the model prediction calculation.

Thermite reduction as an effective metallurgical route for the preparation of TiAl master alloys, which is characterized by green, high efficiency and low energy consumption characteristics, has been discussed in our previous reports [18-21]. Thermodynamic insight into the equilibrium component prediction in the Al-Ti-Ca-oxide system has been discussed, which is suitable for the redox process in which a large number of intermetallics will be generated in the reaction process.

2. Principles for model construction

For pure metal or slag systems, the mass action concentration model has been intensely verified [8-17]. However, for the redox reaction involving the slagging process, the internal phase evolution is also based on the law of mass action, which is actually the coupling process of the molten alloy/metal and slag, and then separation takes place in the presence of a gravity field. Taking the mass action concentration model as the trunk and based on the law of conservation of mass, the alloy and slag are coupled as a whole to predict the phase composition of the equilibrium of chemical reaction at a certain temperature, which is called the extended (or generalized) mass action concentration model (GMACM). The main basis are as follows:

(1) The equilibrium system consists of atoms, ions and molecules (compounds);

(2) A dynamic equilibrium exists among the components in the system, which is displayed as

$$xA + yB \overset{dynamic\ equilibrium}{\Leftrightarrow} AxBy \quad \text{(Alloy)} \quad (1)$$

$$x\left(\frac{2}{n}Me^{n+} + O^{2-}\right) + yC \overset{dynamic\ equilibrium}{\Leftrightarrow} MeO_xC_y \quad \text{(Slag)} \quad (2)$$

where A, B, Me and C represent the metal atoms, metal ions and molecular compounds, respectively.

(3) The chemical reaction in the system obeys the law of mass action, while the structural units in the system are subject to the law of mass conservation.

Theoretically, it can be considered that the ensemble of alloy and slag meets the conditions of the mass action concentration model because the theoretical equilibrium of the system is reached at a certain temperature, and then the alloy and slag will be separated from each other due to the difference in physical properties in the subsequent process. Because of the excellent physicochemical properties of calcium aluminate, calcium oxide is usually used as a flux in metallurgical processes. For the melts formed from the Al-TiO_2-$KClO_3$-CaO system, which is the preformed system for fabrication of TiAl alloy with Al as reducing and alloying agent through self-propagating metallurgy, the schematic diagram for separation is shown in Fig. 1.

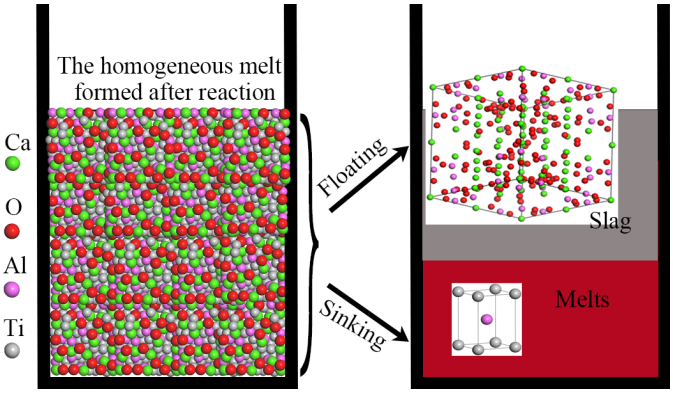

Fig. 1. Schematic diagram of separation between alloy and slag

3. Calculation model for the Al-Ti-Ca-oxide system

For most metallurgical processes, a reducing agent is used to reduce a certain metal from its oxides, sulfides, or corresponding salts to form the corresponding metal or alloy, which is usually accompanied by a reduction and slag-making process. In these processes, volatile substances are released at high temperatures, so models can be built to include volatile components, either from the feedstock or the reaction. For the Al-TiO_2-CaO-$KClO_3$ system, which is the main constituent for the preparation of TiAl alloys through thermite reduction, the experimental details were presented in the previous reports [18,21], and the construction of the calculation model can be listed in the following sections.

3.1. Boundary conditions

According to the thermodynamic calculation, Al, TiO_2 and CaO are used as raw materials to locate the composition of slag in the range of $3CaO \cdot Al_2O_3$ and $CaO \cdot Al_2O_3$, which is the lowest melting point of CaO-Al_2O_3 binary diagram [22]. While the heat generated in the reaction is not enough to maintain spontaneous progress [18,19,23], it is necessary to add a proper amount of substances in a strong exothermic system to improve the heat effect per unit mass (HPM) of the system; here, potassium chlorate is usually used. Considering that $KClO_3$ only provides heat for the system in the reaction process, it can be considered that all KCl generated in the reaction can be volatilized in the form of gas. The corresponding reactions for the preparation of TiAl alloy through SHS metallurgy can be expressed by Eqs. (3)-(6).

$$3TiO_2 + 4Al = 3Ti + 2Al_2O_3 \quad (3)$$

$$3TiO_2 + (4 + 3x)Al = 3TiAl_x + 2Al_2O_3 \quad (4)$$

$$15TiO_2 + 5(4 + 3x)Al + 22CaO = \\ = 15TiAl_x + 4(CaO \cdot Al_2O_3) + 6(3CaO \cdot Al_2O_3) \quad (5)$$

$$KClO_3 + 2Al = KCl\uparrow + Al_2O_3 \quad (6)$$

Eventually, the Al-TiO_2-CaO-$KClO_3$ system can be equivalent to that of Al-TiO_2-CaO-Al_2O_3, and the simplified diagram is shown in Fig. 2.

According to the actual material ratio, the amount of converted substance after the volatile substance is completely removed can be acquired, which can be used as the boundary conditions of GMACM and applied in the equilibrium calculation of the thermite reduction system.

3.2. Structural units in the Al-TiO_2-CaO-Al_2O_3 system

For the reaction system consisting of TiO_2, Al_2O_3, CaO and Al, the structural composition of the melt should be based on the

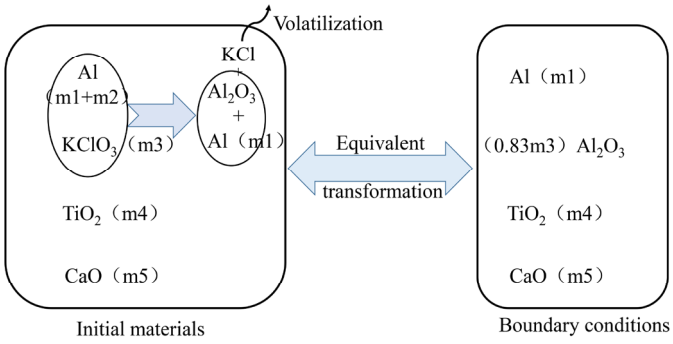

Fig. 2. Equivalent transformation diagram of the initial boundary conditions of GMACM

diagrams of Al-Ti [24], TiO_2-CaO [25], TiO_2-Al_2O_3 [26], and CaO-Al_2O_3 [22], and the system can be regarded as the coupling of the Ti-Al binary system and TiO_2-CaO-Al_2O_3 ternary system when it reaches complete equilibrium. Through the analysis of the phase diagram, the possible structural units of the system are as follows:

(1) Simple components: Ti, Al, O^{2-}, Ca^{2+};
(2) Simple compounds: Ti_3Al, TiAl, $TiAl_2$, $TiAl_3$, Ti_2Al_5, TiO_2, Ti_2O_3, TiO, Ti_3O_5, Ti_4O_7, Ti_9O_{17}, Ti_8O_{15}, Ti_7O_{13}, Ti_6O_{11}, Ti_5O_9, Al_2O_3;
(3) Complex compounds: $TiO_2 \cdot Al_2O_3$, $CaO \cdot TiO_2$, $4CaO \cdot 3TiO_2$, $3CaO \cdot 2TiO_2$, $CaO \cdot Al_2O_3$, $3CaO \cdot Al_2O_3$, $CaO \cdot 2Al_2O_3$, and $CaO \cdot 6Al_2O_3$.

3.3. GMACM for Al-TiO_2-CaO-Al_2O_3 system

The definition of the action concentration of the hybrid system is described in TABLE 1, and the chemical reactions between structural units in the hybrid system are shown in TABLE 2, and the relevant calculation are from Reaction module in the FACTSage software 6.4 along with FactPS and FToxid database.

TABLE 1

Definition of the action concentration of the hybrid Al-TiO_2-CaO-Al_2O_3 system

Structural units	Mole number of structural units	Mass action concentrations, N_i
TiO_2	$n_1 = n_{[TiO_2]}$	$N_1 = N[TiO_2] = n_1/sum(n)$
Al	$n_2 = n_{[Al]}$	$N_2 = N[Al] = n_2/sum(n)$
Ca^{2+}+ O^{2-}	$n_3 = n_{[Ca^{2+}, CaO]} = n_{[O^{2-}, CaO]}$	$N_3 = N[CaO] = 2n_3/sum(n)$
Al_2O_3 Ti Ti_3Al	$n_4 = n_{[Al_2O_3]}$ $n_5 = n_{[Ti]}$ $n_6 = n_{[Ti_3Al]}$	$N_4 = N[Al_2O_3] = n_4/sum(n)$ $N_5 = N[Ti] = n_5/sum(n)$ $N_6 = N[Ti_3Al] = n_6/sum(n)$
TiAl	$n_7 = n_{[TiAl]}$	$N_7 = N[TiAl] = n_7/sum(n)$
$TiAl_2$	$n_8 = n_{[TiAl_2]}$	$N_8 = N[TiAl_2] = n_8/sum(n)$
$TiAl_3$	$n_9 = n_{[TiAl_3]}$	$N_9 = N[TiAl_3] = n_9/sum(n)$
Ti_2Al_5	$n_{10} = n_{[Ti_2Al_5]}$	$N_{10} = N[Ti_2Al_5] = n_{10}/sum(n)$
Ti_2O_3	$n_{11} = n_{[Ti_2O_3]}$	$N_{11} = N[Ti_2O_3] = n_{11}/sum(n)$
TiO	$n_{12} = n_{[TiO]}$	$N_{12} = N[TiO] = n_{12}/sum(n)$
Ti_3O_5	$n_{13} = n_{[Ti_3O_5]}$	$N_{13} = N[Ti_3O_5] = n_{13}/sum(n)$

TABLE 1. Continued

Ti_4O_7	$n_{14} = n_{[Ti_4O_7]}$	$N_{14} = N[Ti_4O_7] = n_{14}/sum(n)$
Ti_5O_9	$n_{15} = n_{[Ti_5O_9]}$	$N_{15} = N[Ti_5O_9] = n_{15}/sum(n)$
Ti_6O_{11}	$n_{16} = n_{[Ti_6O_{11}]}$	$N_{16} = N[Ti_6O_{11}] = n_{16}/sum(n)$
Ti_7O_{13}	$n_{17} = n_{[Ti_7O_{13}]}$	$N_{17} = N[Ti_7O_{13}] = n_{17}/sum(n)$
Ti_8O_{15}	$n_{18} = n_{[Ti_8O_{15}]}$	$N_{18} = N[Ti_8O_{15}] = n_{18}/sum(n)$
Ti_9O_{17}	$n_{19} = n_{[Ti_9O_{17}]}$	$N_{19} = N[Ti_9O_{17}] = n_{19}/sum(n)$
$TiO_2 \cdot Al_2O_3$	$n_{20} = n_{[TiO_2 \cdot Al_2O_3]}$	$N_{20} = N[TiO_2 \cdot Al_2O_3] = n_{20}/sum(n)$
$CaO \cdot TiO_2$	$n_{21} = n_{[CaO \cdot TiO_2]}$	$N_{21} = N[CaO \cdot TiO_2] = n_{21}/sum(n)$
$4CaO \cdot 3TiO_2$	$n_{22} = n_{[4CaO \cdot 3TiO_2]}$	$N_{22} = N[4CaO \cdot 3TiO_2] = n_{22}/sum(n)$
$3CaO \cdot 2TiO_2$	$n_{23} = n_{[3CaO \cdot 2TiO_2]}$	$N_{23} = N[3CaO \cdot 2TiO_2] = n_{23}/sum(n)$
$CaO \cdot Al_2O_3$	$n_{24} = n_{[CaO \cdot Al_2O_3]}$	$N_{24} = N[CaO \cdot Al_2O_3] = n_{24}/sum(n)$
$3CaO \cdot Al_2O_3$	$n_{25} = n_{[3CaO \cdot Al_2O_3]}$	$N_{25} = N[3CaO \cdot Al_2O_3] = n_{25}/sum(n)$
$CaO \cdot 2Al_2O_3$	$n_{26} = n_{[CaO \cdot 2Al_2O_3]}$	$N_{26} = N[CaO \cdot 2Al_2O_3] = n_{26}/sum(n)$
$CaO \cdot 6Al_2O_3$	$n_{27} = n_{[CaO \cdot 6Al_2O_3]}$	$N_{27} = N[CaO \cdot 6Al_2O_3] = n_{27}/sum(n)$

TABLE 2

Expression of chemical reactions, standard Gibbs free energy, equilibrium constants and mass action concentrations

Reactions	**ΔG^{θ} (J/mol)**	**N_i**
$TiO_2 + 4/3Al = Ti + 2/3Al_2O_3$	$-184944.5 + 40.93T^*$	$N_5 = K_1{*}N_1{*}N_2^{4/3}{*}N_4^{-2/3}$
$3TiO_2 + 5Al = Ti_3Al + 2Al_2O_3$	$-584467 + 129.498T$[27]	$N_6 = K_2{*}N_1^{3}{*}N_2^{5}{*}N_4^{-2}$
$TiO_2 + 7/3Al = TiAl + 2/3Al_2O_3$	$-277700.2 + 64.53T^*$	$N_7 = K_3{*}N_1{*}N_2^{7/3}{*}N_4^{-2/3}$
$TiO_2 + 10/3Al = TiAl_2 + 2/3Al_2O_3$	$-228803 + 51.95T$[27]	$N_8 = K_4{*}N_1{*}N_2^{10/3}{*}N_4^{-2/3}$
$TiO_2 + 13/3Al = TiAl_3 + 2/3Al_2O_3$	$-372623.3 + 106.67T^*$	$N_9 = K_5{*}N_1{*}N_2^{13/3}{*}N_4^{-2/3}$
$2TiO_2 + 14/3Al = Ti_2Al_5 + 4/3Al_2O_3$	$-410384 + 91.39T$[27]	$N_{10} = K_6{*}N_1^{2}{*}N_2^{14/3}{*}N_4^{-4/3}$
$2TiO_2 + 2/3Al = Ti_2O_3 + 1/3Al_2O_3$	$-179265.3 + 10.87T^*$	$N_{11} = K_7{*}N_1^{2}{*}N_2^{2/3}{*}N_4^{-1/3}$
$TiO_2 + 2/3Al = TiO + 1/3Al_2O_3$	$-156625.6 + 20.38T^*$	$N_{12} = K_8{*}N_1{*}N_2^{2/3}{*}N_4^{-1/3}$
$3TiO_2 + 2/3Al = Ti_3O_5 + 1/3Al_2O_3$	$-176357.03 - 5.227T^*$	$N_{13} = K_9{*}N_1^{3}{*}N_2^{2/3}{*}N_4^{-1/3}$
$4TiO_2 + 2/3Al = Ti_4O_7 + 1/3Al_2O_3$	$-183434.5\text{-}4.33T^*$	$N_{14} = K_{10}{*}N_1^{4}{*}N_2^{2/3}{*}N_4^{-1/3}$
$5TiO_2 + 2/3Al = Ti_5O_9 + 1/3Al_2O_3$	$-186039.6 - 4.82T^*$	$N_{15} = K_{11}{*}N_1^{5}{*}N_2^{2/3}{*}N_4^{-1/3}$
$6TiO_2 + 2/3Al = Ti_6O_{11} + 1/3Al_2O_3$	$-186850.7 - 5.9T^*$	$N_{16} = K_{12}{*}N_1^{6}{*}N_2^{2/3}{*}N_4^{-1/3}$
$7TiO_2 + 2/3Al = Ti_7O_{13} + 1/3Al_2O_3$	$-187210.7 - 6.86T^*$	$N_{17} = K_{13}{*}N_1^{7}{*}N_2^{2/3}{*}N_4^{-1/3}$
$8TiO_2 + 2/3Al = Ti_8O_{15} + 1/3Al_2O_3$	$-186600.5 - 8.21T^*$	$N_{18} = K_{14}{*}N_1^{8}{*}N_2^{2/3}{*}N_4^{-1/3}$
$9TiO_2 + 2/3Al = Ti_9O_{17} + 1/3Al_2O_3$	$-188484.3 - 7.56T^*$	$N_{19} = K_{15}{*}N_1^{9}{*}N_2^{2/3}{*}N_4^{-1/3}$
$TiO_2 + Al_2O_3 = TiO_2 \cdot Al_2O_3$	$47563.987 - 31.41T^*$	$N_{20} = K_{16}{*}N_1{*}N_4$
$(Ca^{2+} + O^{2-}) + TiO_2 = CaO \cdot TiO_2$	$-80140 - 6.302T$[28]	$N_{21} = K_{17}{*}N_1{*}N_3$
$4(Ca^{2+} + O^{2-}) + 3TiO_2 = 4CaO \cdot 3TiO_2$	$-243473\text{-}25.758T$[28]	$N_{22} = K_{18}{*}N_1^{3}{*}N_3^{4}$
$3(Ca^{2+} + O^{2-}) + 2TiO_2 = 3CaO \cdot 2TiO_2$	$-164217 - 16.838T$[28]	$N_{23} = K_{19}{*}N_1^{2}{*}N_3^{3}$
$(Ca^{2+} + O^{2-}) + Al_2O_3 = CaO \cdot Al_2O_3$	$-19034.8 - 19T^*$	$N_{24} = K_{20}{*}N_3{*}N_4$
$3(Ca^{2+} + O^{2-}) + Al_2O_3 = 3CaO \cdot Al_2O_3$	$-16156.128 - 29.33T^*$	$N_{25} = K_{21}{*}N_3^{3}{*}N_4$
$(Ca^{2+} + O^{2-}) + 2Al_2O_3 = CaO \cdot 2Al_2O_3$	$-23376.124 - 27.029T^*$	$N_{26} = K_{22}{*}N_3{*}N_4^{2}$
$(Ca^{2+} + O^{2-}) + 6Al_2O_3 = CaO \cdot 6Al_2O_3$	$-24817.67 - 30.6T^*$	$N_{27} = K_{23}{*}N_3{*}N_4^{6}$

* Calculated by FACTSage 6.4.

Based on the conservation of element mass in the reaction system, the balanced relationships are concluded as follows:

$$N_1 + N_2 + N_3 + N_4 + N_5 + N_6 + N_7 + N_8 + N_9 + N_{10} + N_{11} + N_{12} + N_{13} + N_{14} + N_{15} + N_{16} + N_{17} + N_{18} + N_{19} + N_{20} + N_{21} + N_{22} + N_{23} + N_{24} + N_{25} + N_{26} + N_{27} - 1 = 0 \quad (7)$$

$$(N_1 + N_5 + 3N_6 + N_7 + N_8 + N_9 + 2N_{10} + 2N_{11} + N_{12} + 3N_{13} + 4N_{14} + 5N_{15} + 6N_{16} + 7N_{17} + 8N_{18} + 9N_{19} + N_{20} + N_{21} + 3N_{22} + 2N_{23}) \times sum(n) - n_1 = 0$$
(mass conservation of TiO_2) (8)

$$(N_2 + N_6 + N_7 + 2N_8 + 3N_9 + 5N_{10}) \times sum(n) - n_2 = 0$$
(mass conservation of Al) (9)

$$(0.5N_3 + N_{21} + 4N_{22} + 3N_{23} + N_{24} + 3N_{25} + N_{26} + N_{27}) \times sum(n) - n_3 = 0$$
(mass conservation of CaO) (10)

$$(N_4 + N_{20} + N_{24} + N_{25} + 2N_{26} + 6N_{27}) \times sum(n) - n_4 = 0$$
(mass conservation of Al_2O_3) (11)

$$K_1{*}N_1{*}N_2^{4/3}{*}N_4^{-2/3} - N_5 = 0 \quad (12)$$

$$K_2*N_1^3*N_2^5*N_4^{-2} - N_6 = 0 \quad (13)$$

$$K_3*N_1*N_2^{7/3}*N_4^{-2/3} - N_7 = 0 \quad (14)$$

$$K_4*N_1*N_2^{10/3}*N_4^{-2/3} - N_8 = 0 \quad (15)$$

$$K_5*N_1*N_2^{13/3}*N_4^{-2/3} - N_9 = 0 \quad (16)$$

$$K_6*N_1^2*N_2^{14/3}*N_4^{-4/3} - N_{10} = 0 \quad (17)$$

$$K_7*N_1^2*N_2^{2/3}*N_4^{-1/3} - N_{11} = 0 \quad (18)$$

$$K_8*N_1*N_2^{2/3}*N_4^{-1/3} - N_{12} = 0 \quad (19)$$

$$K_9*N_1^3*N_2^{2/3}*N_4^{-1/3} - N_{13} = 0 \quad (20)$$

$$K_{10}*N_1^4*N_2^{2/3}*N_4^{-1/3} - N_{14} = 0 \quad (21)$$

$$K_{11}*N_1^5*N_2^{2/3}*N_4^{-1/3} - N_{15} = 0 \quad (22)$$

$$K_{12}*N_1^6*N_2^{2/3}*N_4^{-1/3} - N_{16} = 0 \quad (23)$$

$$K_{13}*N_1^7*N_2^{2/3}*N_4^{-1/3} - N_{17} = 0 \quad (24)$$

$$K_{14}*N_1^8*N_2^{2/3}*N_4^{-1/3} - N_{18} = 0 \quad (25)$$

$$K_{15}*N_1^9*N_2^{2/3}*N_4^{-1/3} - N_{19} = 0 \quad (26)$$

$$K_{16}*N_1*N_4 - N_{20} = 0 \quad (27)$$

$$K_{17}*N_1*N_3 - N_{21} = 0 \quad (28)$$

$$K_{18}*N_1^3*N_3^4 - N_{22} = 0 \quad (29)$$

$$K_{19}*N_1^2*N_3^3 - N_{23} = 0 \quad (30)$$

$$K_{20}*N_3*N_4 - N_{24} = 0 \quad (31)$$

$$K_{21}*N_3^3*N_4 - N_{25} = 0 \quad (32)$$

$$K_{22}*N_3*N_4^2 - N_{26} = 0 \quad (33)$$

$$K_{23}*N_3*N_4^6 - N_{27} = 0 \quad (34)$$

In order to eliminate the total mole amount [sum(n)] in the calculation process, (35)~(37) can be obtained from equations (8)~(11):

$$(N_1 + N_5 + 3N_6 + N_7 + N_8 + N_9 + 2N_{10} + 2N_{11} + N_{12} + 3N_{13} + 4N_{14} + 5N_{15} + 6N_{16} + 7N_{17} + 8N18 + 9N_{19} + N_{20} + N_{21} + 3N_{22} + 2N_{23}) \times n_2 = (N_2 + N_6 + N_7 + 2N_8 + 3N_9 + 5N_{10}) \times n_1 \quad (35)$$

$$(N_1 + N_5 + 3N_6 + N_7 + N_8 + N_9 + 2N_{10} + 2N_{11} + N_{12} + 3N_{13} + 4N_{14} + 5N_{15} + 6N_{16} + 7N_{17} + 8N_{18} + 9N_{19} + N_{20} + N_{21} + 3N_{22} + 2N_{23}) \times n_3 = (0.5N_3 + N_{21} + 4N_{22} + 3N_{23} + N_{24} + 3N_{25} + N_{26} + N_{27}) \times n_1 \quad (36)$$

$$(N_1 + N_5 + 3N_6 + N_7 + N_8 + N_9 + 2N_{10} + 2N_{11} + N_{12} + 3N_{13} + 4N_{14} + 5N_{15} + 6N_{16} + 7N_{17} + 8N_{18} + 9N_{19} + N_{20} + N_{21} + 3N_{22} + 2N_{23}) \times n_4 = (N_4 + N_{20} + N_{24} + N_{25} + 2N_{26} + 6N_{27}) \times n_1 \quad (37)$$

GMACM is composed of equations (7) and (11)-(37) above for the Al-TiO_2-CaO-Al_2O_3 system. Obviously, N_1~N_{27}, n_1, n_2, n_3 and n_4 in the equations are to be calculated, among which n_1, n_2, n_3 and n_4 can be determined after the determination of the initial condition. Furthermore, as a set of software packages for mathematical optimization analysis and synthesis, First Optimization 1.5 (1 stOpt, 7D-Soft High Technology Inc.) program software with the Simplex Method was used to acquire the solutions of these nonlinear equations in calculating model, the admissible error of convergence is 1×10^{-10}, and the judgement times of admissible error of convergence is no less than 1000, then the calculation model was solved.

4. Results and discussion

4.1. The prediction of slag components with different R(CaO/Al_2O_3)

According to the coupling calculation model established in Section 3, the structural units and the corresponding theoretical contents can be acquired with different ratios of raw materials. For these structural units with concentrations lower than 10^{-3} in the equilibrium Al-TiO_2-CaO-Al_2O_3 system, the effect can be neglected for overdilution in melts. The physicochemical properties of CaO-Al_2O_3 binary clinker are usually determined by the mass ratio between calcium oxide and alumina in the slag, R(CaO/Al_2O_3), which usually determines the interfacial tension, melting point, viscosity and density that affect the separation effect between alloy and slag. The variation of relative molar content curves of the structural units in slag along with various R(CaO/Al_2O_3) in Al-TiO_2-CaO-Al_2O_3 system at 1800 K were acquired, which is displayed in Fig. 3.

As shown in Fig. 3, the amount of dissociative CaO in slag increases rapidly with R(CaO/Al_2O_3) in the range of 0.05-1.0,

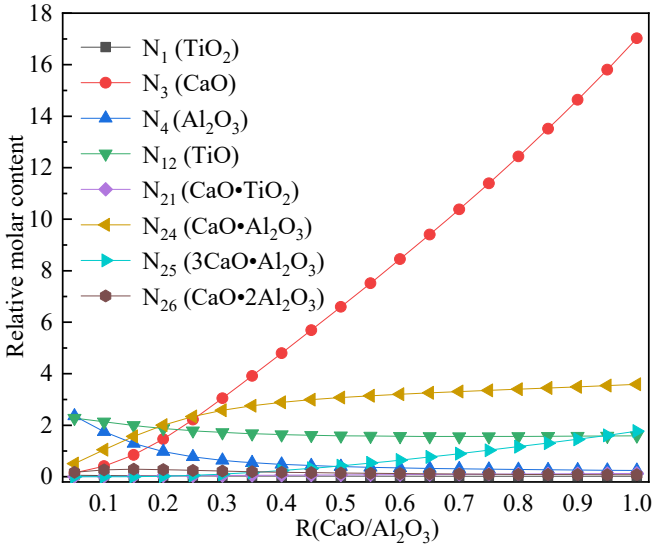

Fig. 3. Variation for the relative molar content of the structural units in slag along with R(CaO/Al_2O_3) in the Al-TiO_2-CaO-Al_2O_3 system at 1800 K

and the growth rate in the second half is greater. The amount of dissociative Al_2O_3 in slag decreases with increasing CaO, while the amount of $CaO \cdot Al_2O_3$ first increases and then tends to be stable. $3CaO \cdot Al_2O_3$ appears when the ratio of $R(CaO/Al_2O_3)$ is greater than 0.3 and further increases with increasing CaO addition. $CaO \cdot 2Al_2O_3$ exists in a small amount in the whole range, and its relative content begins to decrease when $R(CaO/Al_2O_3)$ is greater than 0.3. In addition, in the whole composition range of slag, the relative molar content of TiO shows a slow decreasing trend, while the variation is not obvious, which shows that the reduction of TiO_2 basically does not improve with the variation of $R(CaO/Al_2O_3)$, and the addition of CaO mainly affects the composition of slag. According to the CaO-Al_2O_3 binary diagram, with the increase in the CaO addition coefficient, the evolution trend of slag is $CaO \cdot 2Al_2O_3 \rightarrow CaO \cdot Al_2O_{33} \rightarrow 3CaO \cdot Al_2O_3$. However, when the amount of CaO is further increased, the amount of dissociative CaO in the slag is significantly increased. Combined with the melting point of phases in calcium aluminate, when the composition point of the phase falls between $CaO \cdot Al_2O_3$ and $3CaO \cdot Al_2O_3$ in the binary system, the melting point is relatively low, and the viscosity of slag is low at the same smelting temperature with good liquidity. Furthermore, because the experimental process involves batching error, the inevitable loss in the mixing process and the current situation in which the reaction has difficulty reaching the theoretical equilibrium state, the actual chemical reaction is always carried out under the condition of deviating away from the theoretical value. A large amount of chemical heat generated in the reaction process is transmitted into the surrounding environment owing to the presence of a temperature difference, which makes the system temperature uncontrollably drop too fast, resulting in the condensation of some alloys and slag before its separation process. As a result, these comprehensive factors made the actual batching always deviate from the optimal theoretical point. Moreover, it can be concluded that the variation of $R(CaO/Al_2O_3)$ has little effect on the alloy components, while the properties of the slag mainly affect the difficulty of the separation between alloy and slag, and the composition of alloy is determined by the reducing agent and alloying agent in the raw materials.

Information on the potential phase evolution in the metallurgical process can be attained by the change in the composition of oxides in the slag under reduction conditions. The structural unit $N_{12}(TiO)$ reflects the reduction degree of TiO_2, $N_{21}(CaO \cdot TiO_2)$ reflects the mineralization of TiO_2 because of the addition of lime, and $N_{24}(CaO \cdot Al_2O_3)$ and $N_{25}(3CaO \cdot Al_2O_3)$ reflect the location for the melting point of slag in the binary diagram of the CaO-Al_2O_3 system. The variation trend of slag composition with various $R(CaO/Al_2O_3)$ are shown in Fig. 4, the content of $N_{12}(TiO)$ in the system displays an opposite tendency with $R(CaO/Al_2O_3)$ and increases with temperature, indicating that increasing the temperature in the actual process is not conducive to the reduction of titanium oxide. Combined with the variation trend of $N_{24}(CaO \cdot Al_2O_3)$ and $N_{25}(3CaO \cdot Al_2O_3)$, $N_{25}(3CaO \cdot Al_2O_3)$ appears in the slag with $R(CaO/Al_2O_3)$ is above 25%. Meanwhile, $N_{24}(CaO \cdot Al_2O_3)$ reaches the highest point when $R(CaO/Al_2O_3)$ above 40%, and its content decreases with a further increase in $R(CaO/Al_2O_3)$. Therefore, it further indicates that the appropriate $R(CaO/Al_2O_3)$ interval should be between 30% and 60%. The reduction and slag-making processes are all exothermic, and the change in temperature will affect the reaction equilibrium. In order to explain the variation law of slag composition with $R(CaO/Al_2O_3)$, SHS experiments under different $R(CaO/Al_2O_3)$ values are carried out. The experimental details are described in detail in our previous report [18], and the $R(CaO/Al_2O_3)$ can be regulated by adjusting the ratio of raw materials. Moreover, with the increase of $R(CaO/Al_2O_3)$, that is, CaO was continuously added in the batching process, $CaO \cdot 6Al_2O_3$ and $CaO \cdot 2Al_2O_3$ in the slag after reaction gradually decrease until disappear, while $CaO \cdot Al_2O_3$ and $12CaO \cdot 7Al_2O_3$ appear and gradually increase. The mineralization of TiO_2 increases with $R(CaO/Al_2O_3)$ and temperature from the variation trend of $N_{21}(CaO \cdot TiO_2)$; however, this effect is not significant overall and can be ignored in the experimental process.

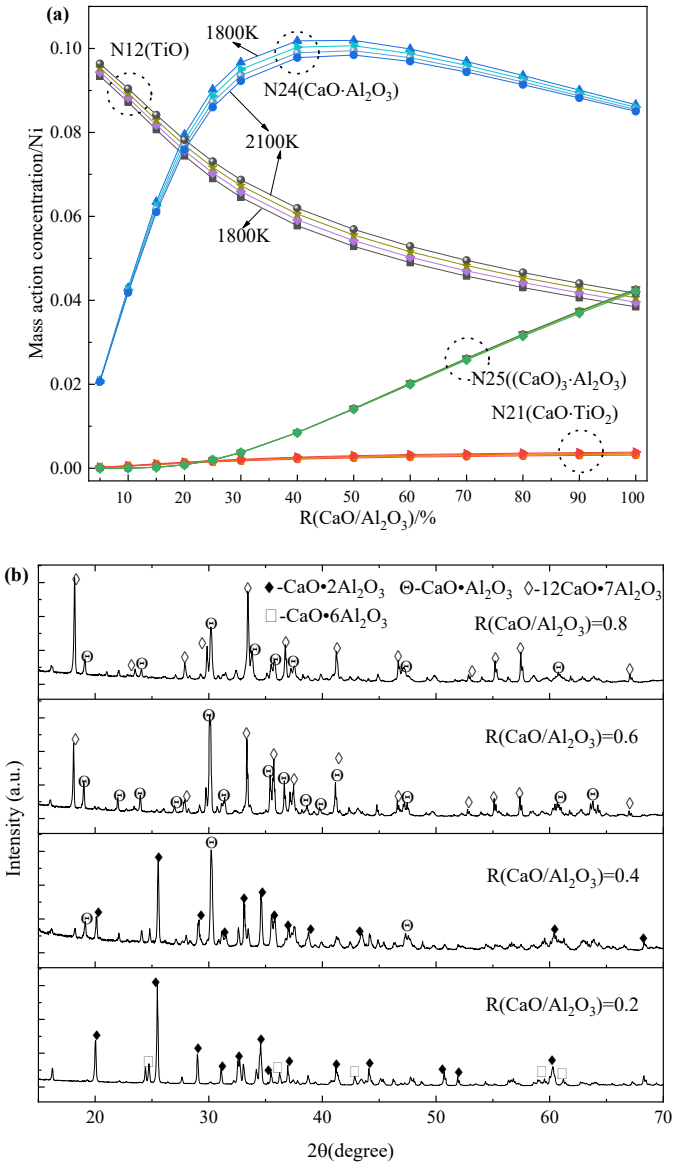

Fig. 4. The variation of slag composition with various $R(CaO/Al_2O_3)$

4.2. Effect of reducing agent addition

For the preparation of intermetallic compounds or alloys through the aluminothermic route, aluminum acts as both a reducing agent and an alloying agent. The typical characteristic of such reactions is that the synthesized intermetallic compounds change the aluminum content of the alloy, especially for these elements in the alloy are easily combined, and the amount of aluminum in the raw material is not easy to control. Based on the calculation results with aluminum addition coefficient at the range of 60%-100%, the phases present in melts are N_2(Al), N_5(Ti), N_6(Ti_3Al), N_7(TiAl), N_8($TiAl_2$), N_9($TiAl_3$) and N_{10}(Ti_2Al_5), and display different trends with the variation in the aluminum addition coefficient (Fig. 5a). Comparing the calculated values with the experimental results acquired from chemical titration analysis, the variation trend of the aluminum content in alloy is consistent within the whole range of aluminum addition coefficients.

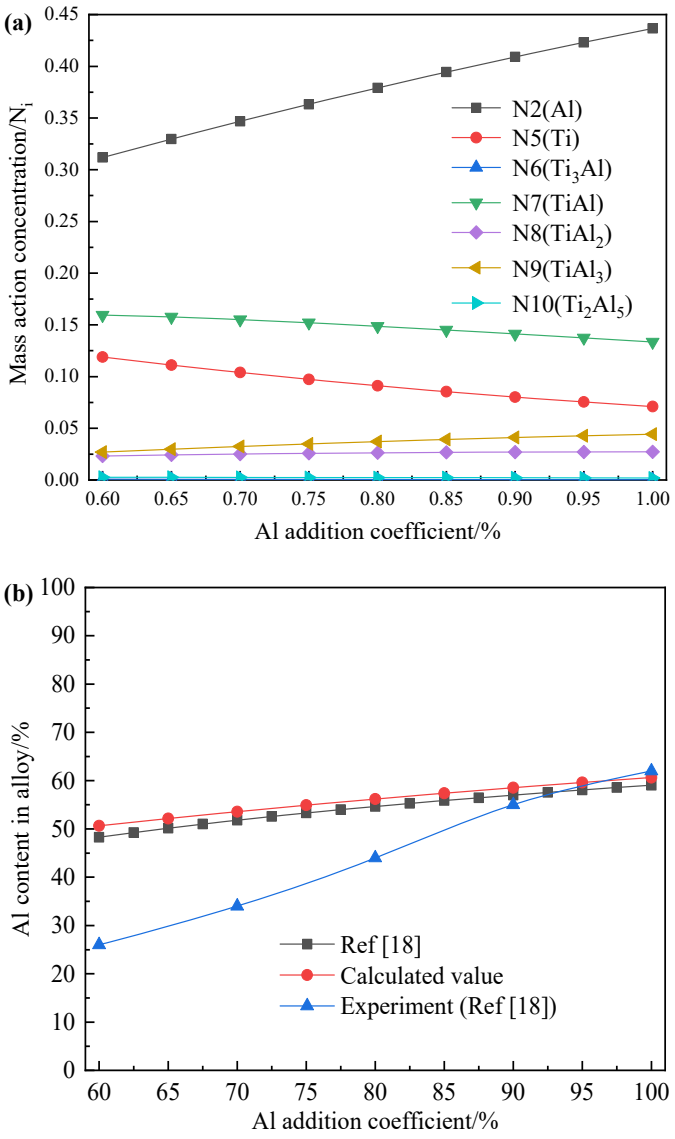

Fig. 5. The existing phases and their contents in alloys with different Al addition coefficients (a), comparison between calculation and experiments (b) at 1800 K

In addition, by comparing the content of alloy composition under different aluminum addition conditions, it can be seen that the experimental and theoretical predictions are close in the high aluminum zone, while the difference is relatively large in the low aluminum zone, and it is similar to the theoretical results presented in Ref. [18] (Fig. 5b). The reason for this difference is not only related to the difference in reducing ability caused by the different additions of reducing agent, but also related to the output of alloy. It is generally believed that the separation between alloy and slag will correspondingly increase when alloy production is large, which slows the cooling rate of the molten pool and prolongs the cooling and solidification time. At the same time, the increase in alloy content also increases the collision probability among metal droplets in the slag, which is more conducive to the collision, growth and sinking process of metal droplets in the slag.

Furthermore, the separation effect between slag and metal also influenced by reaction kinetics, which is usually exhibited through the physicochemical properties of molten slags and the alloy/slag ratio. Generally, measures taken, including the usage of Ca-containing compound reducing agents and the appropriate lowering of lime consumption can be used to promote the precipitation of alloys, all of which can be incorporated into the constructed equilibrium component prediction model. Therefore, the model is suitable for most metallurgical processes including redox and slagging, and can be used for predicting the approximate ratio range of raw materials.

5. Conclusions

In this paper, a modified mass action concentration model for predicting the composition of Al-Ti-Ca-oxide system originates from redox and slag-making reactions is proposed. The modified mass action concentration model based on the law of interaction and mass conservation provides a novel alternative route to determine the proportion of metallurgical raw materials through continuous experiments. The appropriate R(CaO/Al_2O_3) interval in the Al-Ti-Ca-oxide system with an optimized physicochemical properties of slags should be located between 30% and 60%, moreover, the reduction and slagging processes are all exothermic, and the change in temperature will affect the reaction equilibrium. Based on this modified model, the equilibrium relationship between raw materials and products under specific conditions can be constructed, which can be used to reducing the cost of the experiment for predicting the operability of the actual process.

Acknowledgements

This research was financially supported by the Doctoral Scientific Research Founds of Liaocheng University (Grant NO. 318052124), National Natural Science Foundation of China (Grant NO. U1908225) and the Second Batch of Industry University Cooperation and Collaborative Education Projects of the Ministry of Education (Grant NO. 202102251007).

REFERENCES

[1] S.C. Duan, X. Shi, M.T. Mao, W.S. Yang, S.W. Han, H.J. Guo, J. Guo, Sci. Rep. **8**, 5232 (2018). DOI: https://doi.org/10.1038/s41598-018-23556-3

[2] C. Wang, J.J. Zhao, X.Y. Wang, H.S. Zhou, J.F. Xu, K. Wan, Hot Working Technology **43** (17), 70-72 (2014).

[3] J. Zhang, P. Wang, Calphad **25** (3), 343-354 (2001). DOI: https://doi.org/10.1016/S0364-5916(01)00054-2

[4] H. Saxen, M.A. Ramírez-Argáez, A. Conejo, A. Dutta, Processes **9** (2), 252 (2021). DOI: https://doi.org/10.3390/pr9020252

[5] Q.R. Tian, G.C. Wang, D.L. Shang, H. Lei, X.H. Yuan, Q. Wang, J. Li, Metall. Mater. Trans. B **49** (6), 3137-3150 (2018). DOI: https://doi.org/10.1007/s11663-018-1411-8

[6] A.A. Llamas, A.V. Delgado, A.V. Capilla, C.T. Cuadra, M. Hultgren, M. Peltomäki, A. Roine, M. Stelter, M.A. Reuter, Miner. Eng. **131** (15), 51-65 (2019). DOI: https://doi.org/10.1016/j.mineng.2018.11.007

[7] C.B. Shi, X.M. Yang, J.S. Jiao, C. Li, H.J. Guo, ISIJ Int. **50** (10), 1362-1372 (2010). DOI: https://doi.org/10.2355/isijinternational.50.1362

[8] Z.L. Zuo, Q.B. Yu, J.X. Liu, Q. Qin, H.Q. Xie, F. Yang, W.J. Duan, ISIJ Int. **57** (2), 220-227 (2017). DOI: https://doi.org/10.2355/isijinternational.ISIJINT-2016-402

[9] H.Y. Tang, T. Wu, J.S. Li, C.B. Ji, Metall. Res. Technol. **112** (4), 409-423 (2015). DOI: https://doi.org/10.1051/metal/2015029

[10] P. Wang, W.T. Ma, J. Zhang, Iron and Steel **31** (6), 27-31 (1996).

[11] J. Zhang, Trans. Nonferrous Met. Soc. China **5** (2), 16-22 (1995).

[12] J. Zhang, J. Univ. Sci. Technol. Beijing (English Edition) **5** (4), 208-211 (1998).

[13] J. Zhang, J. Univ. Sci. Technol. Beijing (English Edition) **6** (1), 11-14 (1999).

[14] J. Zhang, J. Univ. Sci. Technol. Beijing (English Edition) **7** (4), 246-250 (2000).

[15] J. Zhang, J. Iron Steel Res. Int. **10** (2), 5-9 (2003).

[16] X.M. Yang, W.J. Zhao, H.J. Guo, Q. Zhang, J. Zhang, Inter. J. Miner. Metall. Mater. **17** (5), 546-557 (2010). DOI: https://doi.org/10.1007/s12613-010-0356-y

[17] A. Avdeef, Eur. J. Pharm. Sci. **110** (15), 2-18 (2017). DOI: https://doi.org/10.1016/j.ejps.2017.03.049

[18] Y.L. Song, Z.H. Dou, T.A. Zhang, Y. Liu, J. Alloys Compd. **789**, 266-275 (2019). DOI: https://doi.org/10.1016/j.jallcom.2019.03.050

[19] Y.L. Song, Z.H. Dou, T.A. Zhang, Y. Liu, L.P. Niu, Rare Met. Mater. Eng. **49** (3), 1015-1019 (2020).

[20] Y.L. Song, Z.H. Dou, T.A. Zhang, Y. Liu, Miner. Process. Extr. M. **42** (8), 535-551 (2021). DOI: https://doi.org/10.1080/08827508.2020.1793145

[21] Y.L. Song, Z.H. Dou, T.A. Zhang, G.C. Wang, J. Mater. Eng. Perform. **30**, 9315-9325 (2021). DOI: https://doi.org/10.1007/s11665-021-06074-8

[22] B. Hallstedl, J. Am. Ceram. Soc. **73**, 15-23 (1990). DOI: https://doi.org/10.1111/j.1151-2916.1990.tb05083.x

[23] I.G. Sharma, S.P. Chakraborty, A.K. Suri, J. Alloys Compd. **393**, 122-128 (2005). DOI: https://doi.org/10.1016/j.jallcom.2004.09.055

[24] U.R. Kattner, J.C. Lin, Y.A. Chang, Metall. Trans. A **8**, 2081-2090 (1992). DOI: https://doi.org/10.1007/BF02646001

[25] A. Jongejan, A.L. Wilkins, J. Less-Common Met. **20** (4), 273-279 (1970). DOI: https://doi.org/10.1016/0022-5088(70)90001-9

[26] Y. Ohishi, Y. Miyauchi, H. Ohsato, K.I. Kakimoto, Jpn. J. Appl. Phys. **43** (6A), L749-L751 (2004). DOI: https://doi.org/10.1143/JJAP.43.L749

[27] L.M. Peng, J.H. Wang, H. Li, J.H. Zhao, L.H. He, Scripta Mater. **52**, 243-248 (2005). DOI: https://doi.org/10.1016/j.scriptamat.2004.09.010

[28] K.T. Jacob, K.P. Abraham, J. Chem. Thermodynamics **41**, 816-820 (2009). DOI: https://doi.org/10.1016/j.jct.2009.02.001